

Structure–Property Relationships of Photopolymerizable Poly(ethylene glycol) Dimethacrylate Hydrogels

Sheng Lin-Gibson,^{*,†} Ronald L. Jones,[†] Newell R. Washburn,[†] and Ferenc Horkay[‡]

Polymers Division, National Institute of Standards and Technology, Gaithersburg, Maryland 20899-8543, and Section on Tissue Biophysics and Biomimetics, Laboratory of Integrative and Medical Biophysics, NICHD, National Institutes of Health, Bethesda, Maryland 20892

Received June 29, 2004; Revised Manuscript Received January 24, 2005

ABSTRACT: Photopolymerized hydrogels from poly(ethylene glycol) dimethacrylate (PEGDM) and similar derivatives have been extensively used as scaffolds for tissue regeneration and other biological applications. A systematic investigation into the structure and mechanical properties of PEGDM hydrogels was performed to characterize the relationships between the network structure and gel properties. Gels were prepared from oligomers of different molecular masses (1000–8000 g/mol) at various concentrations. Small-angle neutron scattering was used to characterize the structural features of hydrogels with respect to their semidilute solution precursors. A well-defined structural length scale manifested as a maximum in the scattering intensity was observed for hydrogels derived from high molecular mass PEGDMs and/or high oligomer mass fractions. Mechanical testing showed that PEGDM hydrogels are mechanically robust, consistent with gel structures that contain reinforcing cross-linked clusters. Shear moduli were determined for hydrogels swollen to various degrees in water. The concentration dependence of shear modulus for these nonideal hydrogels exhibits a power law behavior with an exponent close to $1/3$.

Introduction

Hydrogels produced by photopolymerization have been investigated extensively as biomaterials in applications such as scaffolds for tissue engineering, as drug delivery carriers, in the prevention of thrombosis, in postoperative adhesion formation, and as coatings for biosensors.¹ The photopolymerization process allows the hydrogel to be generated *in vitro* or *in vivo* from a low-viscosity solution of monomer, oligomer, or low molecular mass polymer (macromer) by a free radical pathway in a minimally invasive manner. The chemical cross-linking results in hydrogels that contain high water contents yet possess mechanical properties similar to those of soft tissues. Another advantage of hydrogels is their high permeability for oxygen, nutrients, and other water-soluble metabolites, making them particularly attractive as scaffolds in tissue engineering applications.

The use of photopolymerized hydrogels as opposed to physical gels such as alginate also allows for the material properties to be more easily tuned. For example, a typical approach to control the hydrogel mechanical properties is by adjusting the network cross-link density. This can be achieved by adjusting the molecular mass of the macromer or by varying the mass percent (or fraction) of macromer in the solutions. The cross-link density in fully swollen networks is directly proportional to the gel modulus and inversely proportional to the swelling.² These are important considerations in tissue engineering since the cross-link density affects transport properties, and the mechanical property determines the materials functional practicality and influences cell behavior.¹ In drug delivery applications, the mesh size can be adjusted to control the drug

release rate by varying the amount of cross-linker and length of precursor chains.³

Photopolymerization may also be used to generate hydrogels *in vivo*. The low-viscosity oligomer solutions may be injected into the targeted site and polymerized subcutaneously into the shape of the damaged tissue.

Several groups have used photopolymerizable poly(ethylene glycol) (PEG)-based hydrogels for preparing tissue engineering scaffolds^{4–7} with the macromer molecular mass⁵ and concentration⁸ as parameters for tailoring the mechanical properties. We have prepared a series of controlled molecular mass (MM) poly(ethylene glycol) dimethacrylates (PEGDMs) of high purity and low polydispersity by both conventional solution chemistry and a microwave-assisted route.⁷ Combined proton nuclear magnetic resonance (¹H NMR) and matrix-assisted laser desorption ionization time-of-flight mass spectrometry (MALDI-TOF MS) demonstrated that high degrees of conversion from PEG-hydroxyl end groups to methacrylate end groups were achieved. PEGDMs were photopolymerized in water or growth medium (in the presence of cells) to form hydrogels. Preliminary studies showed varied mechanical response, but the encapsulated cells were completely viable in hydrogels (PEG precursor molecular mass ranging from 2000 to 8000 g/mol and mass fractions from 10% to 30%) after 2 weeks. While the mechanical properties have been shown to be adjustable, little is known about the structure of the hydrogels used as tissue engineering scaffolds. It is well-known in the polymer community that gels in general are inhomogeneous. The structure should strongly affect the mechanical and diffusion properties, both of which are crucial material parameters in designing appropriate scaffolds.

Small-angle neutron scattering (SANS), along with other characterization techniques, has been used extensively to characterize the structure of gels.^{9–12} There have been attempts to describe/fit the gel scattering data

[†] National Institute of Standards and Technology.

[‡] National Institutes of Health.

* To whom correspondence should be addressed. E-mail: slgibson@nist.gov.

by using two or multiple correlation lengths, with two of the correlation lengths attributed to thermal fluctuations and static polymer concentration fluctuations.^{11–13} Although no theory exists that satisfactorily describes the gel structures, SANS have proven to be an effective method in providing structural information for a number of gel systems. The general approach for probing the mesoscale structure is to compare the excess scattering intensity from gels with respect to the corresponding semidilute solution. Several types of gel structures, resulting from the chemical structures and gel formation process, have been identified based on their scattering characteristics. Gels originating from end-cross-linking of semidilute solutions of long chains have been shown to display comparable scattering signals to semidilute solutions, and at the preparation concentration, the concentration dependence of the correlation length generally follows a power law behavior⁹ $\xi_{\text{gel}} \sim \phi^\alpha$, where ξ_{gel} is the gel correlation length, ϕ is the volume fraction, and the theoretical exponent α in a good solvent is $-3/4$. The exponent has been experimentally determined to be -0.79 for end-cross-linked poly(tetrahydrofuran).¹³ Highly branched star-shaped polymers and end-cross-linked gels with high end-group functionalities have been shown to exhibit a pronounced maximum in the scattering.¹⁴

The purpose of this study was to probe the structure of PEGDM dilute solution, semidilute solutions, and corresponding hydrogels using small-angle neutron scattering. The effects of molecular mass and oligomer mass fraction on the gel structures were determined. The structure of the hydrogels was correlated to the mechanical properties, specifically the shear modulus that was obtained using uniaxial compression testing.

Experimental Section

Materials. PEGDM (875 g/mol), PEG (MM \approx 2000 g/mol (2K), 4000 g/mol (4K), and 8000 g/mol (8K)), methacrylic anhydride, ethyl ether, triethylamine, and D₂O were purchased from Sigma-Aldrich²⁰ and used as received. Dichloromethane was also purchased from Sigma-Aldrich and dried over activated molecular sieves (4 Å) prior to use. Photoinitiator Irgacure 2959 (I2959) was obtained from Ciba Specialty Chemicals and used as received.

Synthesis of PEGDMs and Their Hydrogels. PEGDMs (2K, 4K, and 8K) were prepared by reacting PEGs with methacrylic anhydride as described previously.⁷ A brief summary of the synthesis of a 4K PEGDM is as follows. PEG (5.0 g), 2.2 equiv of methacrylic anhydride, and triethylamine (0.20 mL) was reacted in \approx 15 mL of dichloromethane over freshly activated molecular sieves for 4 days at room temperature. The solution was filtered and precipitated into ethyl ether. The product was collected by filtration and then dried in a vacuum oven prior to use.

The molecular mass and molecular mass distribution were determined using a combination of ¹H NMR and MALDI-TOF MS. The relative uncertainty associated with ¹H NMR and MALDI-TOF MS are 8% and 5%, respectively. MALDI-TOF MS show that the purchased 1K PEGDM has a number-average molecular mass (M_n) of 754 g/mol and an overall methacrylate conversion of \approx 90% (80% of the species having two methacrylate end groups and 20% of the species having one methacrylate end group and one hydroxyl end group). PEGDMs prepared as described above had high conversions and high purity.

Photopolymerized hydrogels were prepared according to a previously described procedure.⁸ PEGDM (mass fraction = 10%, 20%, or 30%) and aqueous I2959 solution (mass fraction = 0.05%) were mixed and cross-linked in water for mechanical testing or in D₂O for the SANS measurements. Photopolym-

erization was achieved using a long wavelength UV source (365 nm, 300 μ W/cm²) for 10 min to obtain cross-linked hydrogels.

Small-Angle Neutron Scattering Measurements. PEGDMs and the I2959 initiator were dissolved in D₂O. Measurements were made in sample cells with quartz windows and a path length of 1 mm. PEGDM solutions (10%, 20%, and 30%) were measured as prepared and subsequently exposed to UV irradiation as specified previously to form hydrogels in the sample cells. Dilute PEGDM solutions (1%) were also measured.

SANS measurements were performed on the NG-7 30 m SANS instrument at the NIST Center for Neutron Research (NCNR). Sample-to-detector distances were 15 m, 2 m, and in some measurements 1 m, and incident wavelengths (λ) of 8.44 Å for the 15 and 2 m configurations and 5 Å for the 1 m configuration were used to give q ranges ($q = 4\pi/\lambda \sin(\theta/2)$) of $0.0016 \text{ \AA}^{-1} < q < 0.0164 \text{ \AA}^{-1}$, $0.0119 \text{ \AA}^{-1} < q < 0.1992 \text{ \AA}^{-1}$, and $0.0382 \text{ \AA}^{-1} < q < 0.5968 \text{ \AA}^{-1}$, respectively. Data were analyzed by established methods with the software provided by the NCNR.¹⁵ Incoherent background has been corrected for data shown.

Uniaxial Compression Testing on Hydrogels. The shear modulus was determined using uniaxial compression measurements performed by a TA.XT2I HR texture analyzer (Stable Micro Systems, UK). This apparatus measures the deformation (± 0.001 mm) as a function of an applied force (± 0.01 N). Cylindrical hydrogels (height 3 mm, diameter 6 mm) were deformed (at constant volume) between two parallel glass plates. The shear modulus (G) was calculated from the nominal stress, σ (force per unit undeformed cross-section), using the equation¹⁶

$$\sigma = G(\Lambda - \Lambda^{-2}) \quad (1)$$

where Λ is the macroscopic deformation ratio ($\Lambda = L/L_0$, L and L_0 are the length of the deformed and undeformed specimen, respectively). Measurements were carried out in triplicates at deformation ratios $0.7 < \Lambda < 1$. No volume changes or barrel distortions were detected.

Results and Discussion

PEGDMs of different molecular masses (approximately 1K, 2K, 4K, and 8K) were used in the current study. Dilute solutions were examined to evaluate the solution structures, and semidilute solutions were used to prepare hydrogels upon UV irradiation. The 1K PEGDM was purchased; PEGDMs with molecular mass of 2K, 4K, and 8K were prepared by the reaction of PEG (hydroxyl end groups) and methacrylic anhydride. The degree of conversion, product purity, molecular mass, and molecular mass distribution for all PEGDMs are important parameters in determining the subsequent gel structures and were measured experimentally (Table 1). Combined analyses of ¹H NMR and MALDI-TOF MS demonstrated that all PEGDMs prepared had high purity, high conversion ($>99\%$ conversion), and narrow polydispersity rendering these as appropriate model compounds for studying the structure–property relationships of hydrogels.

SANS Results. Although all poly(ethylene glycol) (PEG) precursors to PEGDM in the molecular mass range studied are water-soluble, the 1K PEGDM forms

Table 1. Molecular Mass and Molecular Mass Distribution of PEGDMs Determined by ¹H NMR and MALDI-TOF MS

PEG	M_n (NMR), g/mol	M_n (MALDI), g/mol	M_w (MALDI), g/mol	PDI
1K		754	779	1.03
2K	2222	2150	2178	1.01
4K	4486	4165	4199	1.01
8K	8333	8680	8776	1.01

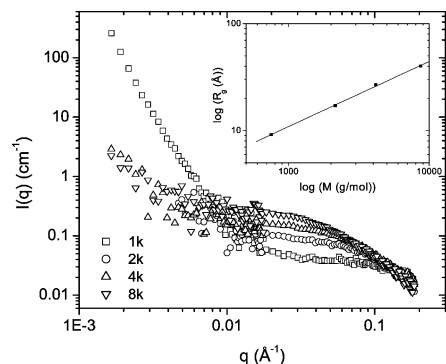


Figure 1. SANS intensity as a function of scattering vector q for dilute (1%) PEGDM solutions. The inset shows the radius of gyration (R_g) as a function of the molecular mass (M).

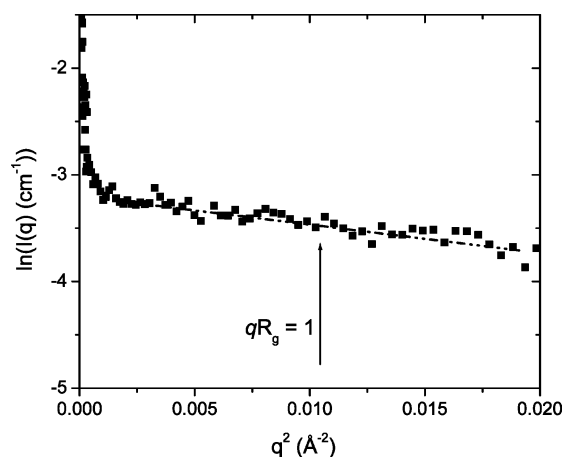


Figure 2. Guinier representation of the scattering intensity $I(q)$ for 1K PEGDM solution (1%). Limit for the Guinier approximation, $qR_g < 1$, is shown.

Table 2. Radius of Gyration (R_g) and Correlation Length (ξ_{sol}) for PEGDM Solutions

PEGDM	dilute solutions		semidilute solutions		
	R_g (Å)	ξ_{sol} (Å)	$\xi_{10\%}$ (Å)	$\xi_{20\%}$ (Å)	$\xi_{30\%}$ (Å)
1K	9.2	7.2			
2K	17.1	8.4	6.6		5.8
4K	26.8	9.5	6.4		5.1
8K	40.2	10.0			

a dispersion. The limited water solubility of the 1K PEGDM is likely due to the relatively high volume fraction of the hydrophobic methacrylate unit. It is therefore of interest to obtain information on the dependence of the association structure or aggregation behavior on the molecular mass of PEGDMs since any structures initially present in the solution may affect the subsequent gel structure. Dilute solutions (mass fraction = 1%) were measured by SANS to probe evidence of aggregation or micelle formation (Figure 1). Only the 1K PEGDM shows a large excess scattering at the low range of wave vector q , indicating the presence of larger structures. In addition, the low q scattering exhibits an apparent power law dependence with a slope of approximately -4 , suggesting the presence of smoothly defined interfaces in the solution. No intensity oscillations are observed, in accordance with highly polydisperse particle sizes.

From the dilute solution measurements, the radii of gyration (R_g) for the PEGDMs are determined from the slope of the Guinier plots ($-R_g^2/3$). Figure 2 illustrates the Guinier analysis of the scattering data for the 1K

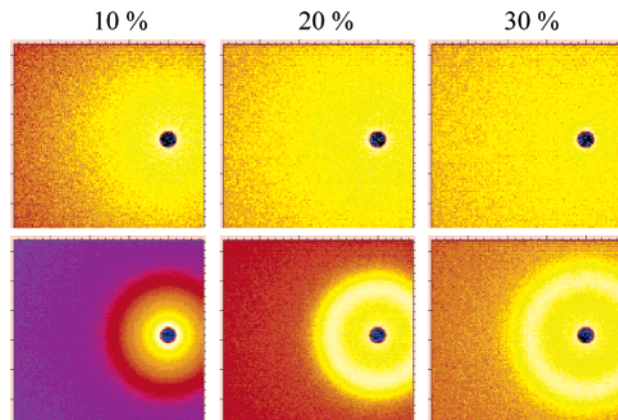


Figure 3. 2-Dimensional scattering patterns of 4K PEGDM solutions (top row) and corresponding gels (bottom row) at various PEGDM mass fractions.

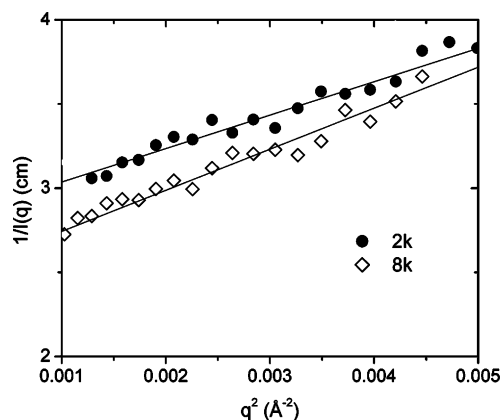


Figure 4. Typical Zimm plots for 10% PEGDM semidilute solutions.

PEGDM solution. The data were fitted in an iterative manner to obtain the best fit inside the Guinier limit. The vertical arrow in the figure indicates the limit for the Guinier approximation ($qR_g < 1$). The excess scattering at low q is likely caused by large inhomogeneities, such as aggregates; therefore, the first few data points were omitted from the analysis. The values of R_g obtained for all four PEGDM samples are listed in Table 2. The slope of the $\log R_g$ vs \log molecular mass plot is 0.61 (inset of Figure 1), consistent with good solvent conditions.

SANS measurements were performed on semidilute PEGDM solutions and corresponding hydrogels made from different oligomer molecular masses at different concentrations. It should be noted that all hydrogels under the current study have reached the maximum methacrylate conversion; i.e., no additional cross-linking occurs upon further UV irradiation. The time required to achieve complete reaction has also been independently determined using in-situ rheology and mechanical testing. Figure 3 shows the 2-dimensional SANS images for the 4K PEGDM solutions and hydrogels of different concentrations. A marked difference can be observed between the solutions and gels. In gels a ring develops, indicating the formation of clusters. This effect is more pronounced at high PEGDM concentrations.

We first examine the semidilute solutions and subsequently infer the structural features of hydrogels. For semidilute solutions, the correlation length (ξ_{sol}) was calculated using a Zimm plot in the Guinier region ($q\xi_{sol} < 1$) in which the slope is proportional to ξ_{sol} and

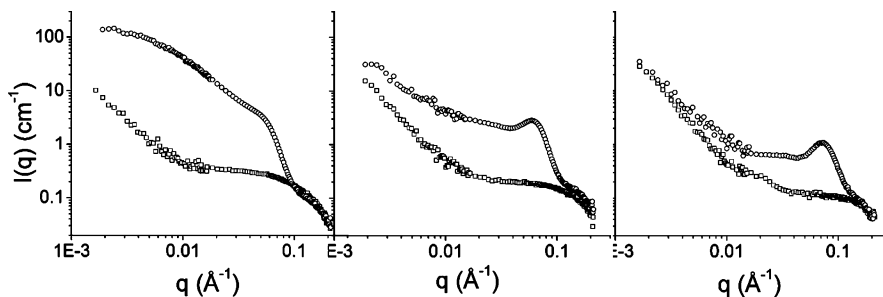


Figure 5. Scattering intensity as a function of the scattering vector for 4K PEGDM solutions (\square) and hydrogels (\circ): 10% (left), 20% (middle), and 30% (right).

depends on the solvent quality (Figure 4). The values are displayed in Table 2. As expected, ξ_{sol} decreases as the concentration increases.

Figure 5 shows the neutron scattering spectra for solutions and corresponding hydrogels prepared from the 4K PEGDM at various concentrations. Differences in the intensity and shape of the curves are clearly visible in the low and intermediate q regions, while the intensity remains practically unchanged in the high q region ($q > 0.12 \text{ \AA}^{-1}$). The latter is expected since the SANS response at high values of q is determined by the local geometry of the polymer chains. In the low q region, a pronounced scattering intensity upturn with a power law dependence is observed for all semidilute solutions. Similar excess scattering intensities at low q , described as the Picot and Benoit effect,¹⁷ have been attributed to transient large-scale concentration fluctuations. The intensity differences in the low q range between solution and gel spectra gradually decrease as the polymer concentration increases. The low q intensity for the 30% solution and gel are comparable, indicating there are essentially no differences between the solution and gel structure at large length scales. In the intermediate q range, the scattering intensity strongly increases upon cross-linking and significantly exceeds that of the corresponding semidilute solution. For hydrogels of high polymer concentrations, a maximum in the scattering intensity at q^* is observed, suggesting the presence of cross-linked clusters with a predominant characteristic length. The q^* for the 20 and 30% hydrogels are 0.059 and 0.073 \AA^{-1} , respectively, corresponding to characteristic lengths ($d = 2\pi/q$) of 106 and 86 \AA , respectively. The scattering spectrum of the 10% hydrogel made from 4K PEGDM chains does not exhibit a maximum but rather a shoulder in the intermediate q range. Although a distinct peak is not available for determining the characteristic length for the 10% hydrogel, the q at which the knee is observed is lower than for the 20% hydrogel, consistent with the notion that the clusters are becoming further apart as the polymer concentration decreases. Similar trends are observed for the 2K PEGDM hydrogels. These results show that the structures are highly dependent on the polymer concentration and illustrate the structural richness of these hydrogels.

Figure 6 shows the neutron scattering spectra of 10% hydrogels prepared from PEGDMs of different molecular masses. It can be seen that the network structure strongly depends on the molecular mass of the precursor polymer chains. The spectrum of 8K PEGDM hydrogel displays a maximum at $q^* \approx 0.032 \text{ \AA}^{-1}$. This implies that the dominant characteristic length of the clusters is approximately 200 \AA . For gels made from shorter chains, the scattering spectra do not exhibit a distinct

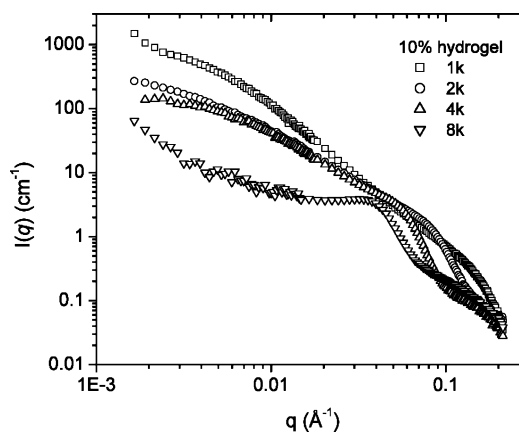


Figure 6. Scattering intensity as a function of the scattering vector for the 10% hydrogels prepared from different molecular mass PEGDMs.

maximum but rather a shoulder that becomes less defined as the molecular mass decreases. Only a broad shoulder is observed for the gel made from the lowest molecular mass (1K) precursor chains. In addition, Figure 6 shows that q^* decreases as molecular mass increases, suggesting that the clusters are becoming farther apart as the molecular mass increases. These results show that the oligomer molecular mass strongly affects both the cluster size and structure.

In general, a distinct maximum in $I(q)$ vs q curve is observed for systems having a soft order, such as those prepared from star-shaped multifunctional cross-linkers.⁹ It has also been reported that the maximum in the scattering spectrum becomes more pronounced as the functionality of the cross-links is increased.¹⁴ In the present case, although the nominal functionality of the PEGDM chains is 4 (2 on each oligomer chain end), the mechanism of the cross-linking process favors the formation of multifunctional junctions. Intermolecular reactions lead to branched structures (Figure 7) similar to those formed in bulk photopolymerization of dimethacrylates.¹⁸ Consequently, it is reasonable to assume that PEGDM hydrogels contain cross-linked clusters embedded in a "solution-like" matrix. As the concentration decreases, the amount of oligomer present becomes insufficient to form uniformly dispersed clusters, thereby creating large "defects" in the network. Large inhomogeneities in the network structure lead to excess scattering intensity at low q . Moreover, the methacrylate-rich domains are diffused and hence appear as a broad shoulder in the SANS results.

Uniaxial Compression Tests. The shear moduli (G) of hydrogels were measured by uniaxial compression and calculated using equations derived from the strain energy function.¹⁹ Figure 8 shows the nominal stress σ

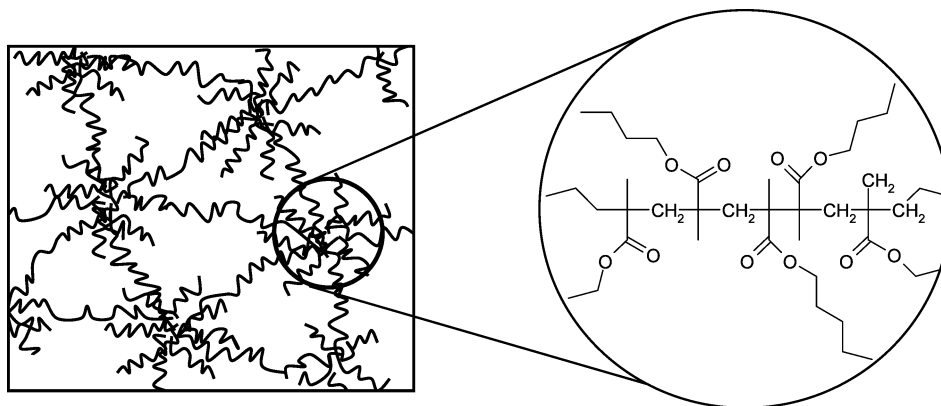


Figure 7. Schematic showing the physical pictures of the PEGDM hydrogels comprised of dense clusters embedded in a weakly cross-linked matrix. The dense clusters are due to cross-linking of methacrylate functionalities, each of which reacts with two methacrylates.

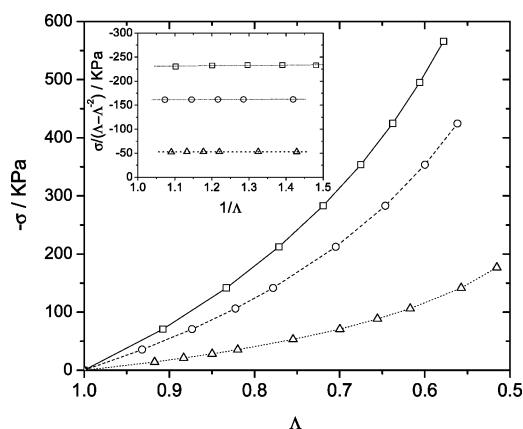


Figure 8. Nominal stress (σ) measured as a function of the deformation ratio (Λ) for 4K PEGDM hydrogels: 10% (Δ), 20% (\circ), and 30% (\square). The inset shows the Mooney–Rivlin representation plotting the reduced stress vs $1/\Lambda$. Note that the σ is negative due to the compressive forces used.

Table 3. Shear Modulus (MPa) for PEGDM Hydrogels Prepared with Different Molecular Mass and at Different Mass PEGDM Mass Fractions

PEGDM	10%	20%	30%
2K	46 ± 5	164 ± 16	297 ± 30
4K	53 ± 5	162 ± 15	233 ± 23
8K	39 ± 4	95 ± 10	169 ± 16

as a function of the deformation ratio Λ for three gels. Note that in compression σ is negative. The inset of Figure 8 plots the normal stress vs the deformation ratio according to the Mooney–Rivlin representation (eq 2).

$$\sigma = 2(\Lambda - \Lambda^{-2})(C_1 + C_2/\Lambda) \quad (2)$$

where C_1 and C_2 are constants. It is apparent that the value of C_2 is approximately zero. This result is consistent with many previous findings reported for swollen polymer networks. $2C_1$ can be identified with the shear modulus of the gels.

The shear moduli of PEGDM hydrogels prepared from different molecular mass oligomers (2K, 4K, and 8K) as a function of PEGDM mass fraction (varying from 10 to 30%) are listed in Table 3. As expected, G monotonically increased as the oligomer mass fraction increased for PEGDMs of all molecular masses. The effect of molecular mass on G appears to depend on the oligomer concentration. For hydrogels made at a high PEGDM mass fraction (30%), the shear modulus de-

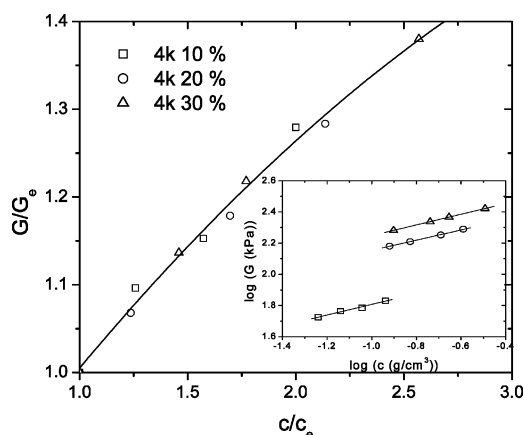


Figure 9. Reduced shear modulus G/G_e as a function of reduced concentration c/c_e for PEGDM gels. The inset shows the variation of G as a function of the polymer concentration (c) for PEGDM hydrogels.

creases as the molecular mass increases due to a decrease in the cross-link density. However, the variation between molecular mass and shear modulus is less pronounced for hydrogels with lower PEGDM contents (i.e., 10 and 20%). Whereas G of hydrogels prepared from the 8K PEGDM are smaller than those prepared from the 2K and 4K PEGDM, there are no significant differences in the G of hydrogels prepared from the 2K and 4K PEGDM at lower polymer concentrations.

As mentioned previously, the gel structure is expected to affect the mechanical properties. Mechanical testing shows that PEGDM hydrogels are mechanically robust, consistent with gel structures that contain cross-linked clusters, which reinforce the networks.

We also attempted to measure the shear modulus of 1K PEGDM hydrogels; however, these hydrogels were brittle, and the results were poorly reproducible. This is not surprising since the network chains are short and the SANS results show that these hydrogels exhibit inhomogeneous structures over the whole range of length scales probed.

Since the hydrogel scaffold is expected to swell (or shrink) in tissue engineering application, it is of interest to examine the effect of swelling on the shear modulus. The 4K PEGDM hydrogels were swollen to various degrees in water, and the shear modulus was measured (inset of Figure 9). As expected, the shear modulus increased as the polymer concentration increased. The slope of the $\log G$ vs $\log c$ curves was between 0.32 and

0.34, consistent with the theory of rubber elasticity, $G = \text{const} \cdot c^{1/3}$. Figure 9 shows the reduced shear modulus G/G_e (where G_e is the shear modulus of the fully swollen hydrogel) as a function of reduced concentration c/c_e (where c_e is the polymer concentration for the fully swollen hydrogel). All data points collapse onto a single curve.

Conclusions

Poly(ethylene glycol) dimethacrylate (PEGDM) chains of controlled molecular mass (between 1K and 8K) and narrow polydispersity were photopolymerized to form hydrogels. Small-angle neutron scattering is used to characterize the structure of hydrogels with respect to their semidilute solution precursors. A well-defined domain size, which appears as a maximum in the scattering intensity, is observed for hydrogels formed from PEGDM with higher oligomer molecular mass and/or high polymer concentration. Hydrogels derived from the lower molecular mass PEGDMs or low oligomer concentrations tend to form polydisperse structures and the domains are diffuse. The physical picture of PEGDM hydrogels is one that consists of dense cross-linked clusters embedded in a "solution-like" matrix.

The network structure clearly affects the shear modulus of the hydrogels. Mechanical testing shows that PEGDM hydrogels are mechanically robust, consistent with gel structures containing reinforcing cross-link clusters. The analysis of hydrogels swollen to various degrees in water indicates that the concentration dependence of the modulus of these highly nonideal gels can be described by a power law with an exponent of approximately $1/3$. The current study demonstrates the subtle balance between oligomer molecular mass and mass fraction in designing hydrogels with desired structures and mechanical properties.

Acknowledgment. Financial support was provided from NIDCR/NIST Interagency Agreement Y1-DE-1021-03. We thank Mr. Sidi Bencherif for his technical assistance.

References and Notes

- (1) Nguyen, K. T.; West, J. L. *Biomaterials* **2002**, *23*, 4307–4314.
- (2) Flory, P. J. *Principles of Polymer Chemistry*; Cornell University Press: Ithaca, NY, 1953.
- (3) Holland, T. A.; Tabata, Y.; Mikos, A. G. *J. Controlled Release* **2003**, *91*, 299–313.
- (4) Seliktar, D.; Zisch, A. H.; Lutolf, M. P.; Wrana, J. L.; Hubbell, J. A. *J. Biomed. Mater. Res., Part A* **2004**, *68A*, 704–716.
- (5) Temenoff, J. S.; Athanasiou, K. A.; LeBaron, R. G.; Mikos, A. G. *J. Biomed. Mater. Res.* **2002**, *59*, 429–437.
- (6) Bryant, S. J.; Anseth, K. S. *J. Biomed. Mater. Res., Part A* **2003**, *64A*, 70–79.
- (7) Lin-Gibson, S.; Bencherif, S.; Cooper, J. A.; Wetzel, S. J.; Antonucci, J. M.; Vogel, B. M.; Horkay, F.; Washburn, N. R. *Biomacromolecules* **2004**, *5*, 1280–1287.
- (8) Bryant, S. J.; Anseth, K. S. *J. Biomed. Mater. Res.* **2002**, *59*, 63–72.
- (9) Bastide, J.; Candau, S. J. Structure of gels as investigated by means of static scattering techniques. In *Physical Properties of Polymeric Gels*; Addad, J. P. C., Ed.; John Wiley & Son: New York, 1996; pp 143–308.
- (10) Hecht, A. M.; Horkay, F.; Geissler, E. *J. Phys. Chem. B* **2001**, *105*, 5637–5642.
- (11) Horkay, F.; Hecht, A. M.; Mallam, S.; Geissler, E.; Rennie, A. R. *Macromolecules* **1991**, *24*, 2896–2902.
- (12) Horkay, F.; Hecht, A. M.; Zrinyi, M.; Geissler, E. *Polym. Gels Networks* **1996**, *4*, 451–465.
- (13) Shibayama, M.; Takahashi, H.; Nomura, S. *Macromolecules* **1995**, *28*, 6860–6864.
- (14) Mendes, E.; Lutz, P.; Bastide, J.; Boue, F. *Macromolecules* **1995**, *28*, 174–179.
- (15) NCNR http://www.ncnr.nist.gov/programs/sans/manuals/data_red.html. 2003. Ref Type: Computer Program.
- (16) Flory, P. J. *Principles of Polymer Chemistry*; Cornell University Press: Ithaca, NY, 1953.
- (17) Koberstein, J. T.; Picot, C.; Benoit, H. *Polymer* **1985**, *26*, 673–681.
- (18) Andrzejewska, E. *Prog. Polym. Sci.* **2001**, *26*, 605–665.
- (19) Treloar, L. R. G. *The Physics of Rubber Elasticity*; Clarendon Press: Oxford, 1975.
- (20) Certain commercial materials and equipment are identified in this paper in order to specify adequately the experimental procedure. In no case does such identification imply recommendation by the National Institute of Standards and Technology nor does it imply that the material or equipment identified is necessarily the best available for this purpose.

MA0487002